

Stratospheric tracer modeling key aspects

B. Bregman et al.

Key aspects of stratospheric tracer modeling

B. Bregman, E. Meijer, and R. Scheele

Royal Netherlands Meteorological Institute, P.O. Box 201, 3730 AE, De Bilt, The Netherlands

Received: 3 February 2006 – Accepted: 7 March 2006 – Published: 6 June 2006

Correspondence to: B. Bregman (bregman@knmi.nl)

Title Page

Abstract

Introduction

Conclusions

References

Tables

Figures

◀

▶

◀

▶

Back

Close

Full Screen / Esc

Printer-friendly Version

Interactive Discussion

EGU

Abstract

This study describes key aspects of global chemistry-transport models and the impact on stratospheric tracer transport. We concentrate on global models that use assimilated winds from numerical weather predictions, but the results also apply to tracer transport in general circulation models. We examined grid resolution, numerical diffusion and dispersion of the winds fields, the meteorology update time intervals, update frequency, and time interpolation. For this study we applied the three-dimensional chemistry-transport Tracer Model version 5 (TM5) and a trajectory model and performed several diagnoses focusing on different transport regimes. Covering different time and spatial scales, we examined (1) polar vortex dynamics during the Arctic winter, (2) the large-scale stratospheric meridional circulation, and (3) air parcel dispersion in the tropical lower stratosphere. Tracer distributions inside the Arctic polar vortex show considerably worse agreement with observations when the model grid resolution in the polar region is reduced to avoid numerical instability. Using time interpolated winds improve the tracer distributions only marginally. Considerable improvement is found when the update frequency of the assimilated winds is increased from 6 to 3 h, both in the large-scale tracer distribution and the polar regions. It further reduces in particular the vertical dispersion of air parcels in the tropical lower stratosphere. The results in this study demonstrates significant progress in the use of assimilated meteorology in chemistry-transport models, which is important for both short- and long-term integrations.

1 Introduction

Global three dimensional chemistry transport models (hereafter referred to as CTMs) driven by actual meteorology from numerical weather predictions are crucial for the interpretation of many observational data. The great advantage is the direct comparison with observations by their ability to utilize actual meteorology to drive the model trans-

ACPD

6, 4375–4414, 2006

Stratospheric tracer modeling key aspects

B. Bregman et al.

Title Page

Abstract

Introduction

Conclusions

References

Tables

Figures

◀

▶

◀

▶

Back

Close

Full Screen / Esc

Printer-friendly Version

Interactive Discussion

EGU

Stratospheric tracer modeling key aspects

B. Bregman et al.

Title Page

Abstract

Introduction

Conclusions

References

Tables

Figures

◀

▶

◀

▶

Back

Close

Full Screen / Esc

Printer-friendly Version

Interactive Discussion

port. CTMs are thus ideally designed for detailed sensitivity studies of key processes important for climate, which would be computationally too expensive for Chemistry-Climate Models (CCMs). Major areas of interest are the polar regions, owing to the prevailing chemical ozone loss during winter and its sensitivity towards climate change, and the tropical region where the main entrance of air into the stratosphere is located (WMO, 2002). The ability of a direct comparison with observations also allows model sensitivity studies to investigate basic model parameters, such as grid resolution and advection schemes, but also the quality of the wind fluxes or vectors and the way the meteorological information is implemented in the CTM.

The impact of grid resolution on the atmospheric composition remains an important subject of discussion. Searle et al. (1998) show that a horizontal resolution of 3° is sufficient to calculate polar chemical ozone loss, but Marchand et al. (2003) in contrast found substantial differences after increasing their model resolution from $2^\circ \times 2^\circ$ to $1^\circ \times 1^\circ$. Another model study also focused on the effect of spatial resolution in the polar region by evaluating methane distributions (van den Broek et al., 2003). An important outcome was the significant overestimation of methane in the lower stratosphere at the edge and inside the polar vortex. An increase of the horizontal grid resolution to $1^\circ \times 1^\circ$ gave negligible improvement and thus indicated very small sensitivity to horizontal resolution. This results support the conclusions from Searle et al. (1998), although the conclusions here were based on long-lived tracer distributions. The results in this study however contrasts these findings.

CTMs and CCMs suffer from numerical instability in regions of strong zonal winds and relatively small grid cells. The most critical regions are located at the poles, in particular during the winter, but also in the vicinity of storm tracks. Negative tracer mass can occur when the transport distance during one advection time step exceeds the size of the grid cell, the so-called Courant-Friedrichs-Lewy (CFL) criterion. Commonly, this is avoided by reducing the grid resolution or by averaging the wind vectors or mass fluxes, but its impact on tracer transport has so far not been investigated.

An obvious solution would be to reduce the advection time step, but this would lead

to excessively small time steps. To overcome this difficulty we introduced an iteration procedure for tracer advection in the TM5 model with locally adjusted time steps (Krol et al., 2005). In Krol et al. (2005) the focus was on the troposphere. In this study we will demonstrate the dramatic impact on the stratospheric tracer distribution.

5 The quality of the winds provided by the numerical weather predictions is another factor affecting tracer transport. The winds are subject to data assimilation within the model prediction and are often referred to as Data Assimilation System or DAS winds (Schoeberl et al., 2002). The quality of particularly the stratospheric winds is affected by the presence of spurious variability or “noise”, inherently introduced through the as-
10 similation procedure, either through a lack of suitable observations or by inaccurate treatment of the model biases. This unwanted variability causes enhanced dispersion that accumulates in time. Hence, the impact of dispersion increases with increasing dynamic time scales. It may therefore not be a serious problem for the troposphere where the dynamic turnover times are relatively short. However, the stratospheric circulation
15 contains much longer time scales where spurious variability in DAS winds becomes very critical. One of the consequences is enhanced dispersion and an enforced large-scale stratospheric meridional circulation, causing tracer residence times to be considerably shorter than observed (Schoeberl et al., 2002; Douglass et al., 2003; Meijer et al., 2004). The most critical region is the tropical lower stratosphere, where the ma-
20 jority of the air enters the stratosphere. Moreover, this is a very complicated region for data assimilation due to a lack of observations and because the atmosphere deviates from geostrophical balance, which complicates proper treatment of model biases.

Meijer et al. (2004) and Scheele et al. (2005) show that the intensity of dispersion in the DAS winds increases when the assimilation procedure is less accurate or less sophisticated. For example, the ECMWF utilizes three- and four-dimensional
25 assimilation procedures (3DVAR and 4DVAR respectively). 4DVAR is a temporal extension of 3DVAR, and thus more accurate but also computationally more expensive. A comprehensive description of the ECMWF assimilation procedures can be found at <http://www.ecmwf.int>. A major difference is that 4DVAR produces physically more bal-

Stratospheric tracer modeling key aspectsB. Bregman et al.

Title Page

Abstract

Introduction

Conclusions

References

Tables

Figures

◀

▶

◀

▶

Back

Close

Full Screen / Esc

Printer-friendly Version

Interactive Discussion

Stratospheric tracer modeling key aspects

B. Bregman et al.

[Title Page](#)[Abstract](#)[Introduction](#)[Conclusions](#)[References](#)[Tables](#)[Figures](#)[◀](#)[▶](#)[◀](#)[▶](#)[Back](#)[Close](#)[Full Screen / Esc](#)[Printer-friendly Version](#)[Interactive Discussion](#)

EGU

anced winds for each model time step, due to the inclusion of time. Because of computational expenses the long-term re-analyses (ERA40) has been performed with 3DVAR, while the operational data, analyses and forecasts (referred to as “Operational Data” or OD) are produced with 4DVAR. Comparing both data sets thus yields information about the impact of assimilation accuracy on tracer transport. Ozone is a useful tracer, since its distribution is very vulnerable to the strength of large-scale stratospheric circulation. [Laat et al. \(2006\)](#) and [van Noije et al. \(2004\)](#) show a very strong accumulation of ozone in the extra-tropical lower stratosphere when using ERA40 winds, resulting in significant overestimation compared to observations. When applying OD winds, the agreement becomes much better. Indeed, [van Noije et al. \(2004\)](#), [Simmons et al. \(2005\)](#) and [Scheele et al. \(2005\)](#) have shown that OD winds contain less dispersion than ERA40 winds in the tropical lower stratosphere and provide more realistic extra-tropical downward ozone fluxes ([van Noije et al., 2004](#)) and more realistic stratospheric residence times ([Meijer et al., 2004](#)). However, even with OD the circulation remains too strong ([Laat et al., 2006](#)), which has led to the practical decision to constrain stratospheric ozone down to 100 hPa in the extra-tropics with ozone climatology ([van Noije et al., 2004](#)) for the tropospheric multi-year IPCC chemistry-transport runs. However for coupled troposphere-stratosphere runs this solution is undesirable.

Recently, a comprehensive model intercomparison was performed with winds and temperatures from a variety of data assimilation systems, focusing on the 2002 Antarctic vortex split ([Manney et al., 2005](#)). They show substantial differences between the models that apply different DAS, with operational (4DVAR) analysis performing better than re-analysis (3DVAR) data, consistent with the studies described above.

Despite shortcomings in ERA40 winds, the dynamical variability can be simulated quite well ([Hadjinicolaou et al., 2005](#); [Chipperfield, 2006](#)). This is in line with a comparison between DAS winds from different numerical weather predictions, where ERA40 winds were found to agree excellent with observed variability ([Randel et al., 2003](#)). It is important to note that instantaneous variability and enhanced dispersion or noise in the winds are two separated issues. The above mentioned studies with ERA40 clearly

demonstrate this.

Recently, we have evaluated forecasts instead of analyses, assuming that forecasts are physically more balanced and thus are expected to contain less noisy winds, similar to the differences between 3DVAR and 4DVAR winds. Indeed, in a recent trajectory study we have shown that by increasing the forecast length the dispersion in the tropical lower stratosphere is significantly reduced (Scheele et al., 2005). In line with these results the mean age of air becomes older in the extra-tropical stratosphere, closer to observations (Meijer et al., 2004). However, it now became too old in the tropical lower stratosphere, while still remaining too young in the extra-tropics.

The representation of the large-scale meridional circulation in the stratosphere by DAS winds considerably improves when using isentropic vertical coordinates and heating rates instead of vertical wind velocity or mass fluxes on pressure levels (Mahowald et al., 2002). Although an isentropic coordinate seems physically more appropriate for stratospheric dynamics, a mass correction needs to be performed in order to balance the divergence with the isentrope tendencies, which will impact the tracer distributions. This is a fundamental mass balance problem that applies to both CTMs and GCMs independent of the vertical coordinate system, as has been demonstrated by Jöckel et al. (2001) and for which different mass fixers have been introduced (cf. Bregman et al., 2003; Rotman et al., 2004). When integrating over a full vertical range from the upper stratosphere to the surface, the isentropic vertical coordinate needs to be adjusted from purely isentropic to a hybrid of pressure and isentropes. So far only two models have inferred such a hybrid coordinate (Mahowald et al., 2002; Chipperfield, 2006), which still contain mass imbalance issues but are promising developments.

By applying the algorithm of Segers et al. (2002), Bregman et al. (2003) have shown that the use of mass fixers can be avoided by applying mass-flux advection, without violating mass conservation. This is a fundamental underlying aspect in this study. We have demonstrated complete mass conservation using the hybrid sigma-pressure coordinate, while so far this has not been proven for other vertical coordinate systems.

Hybrid sigma-pressure remains a very practical vertical coordinate for global tracer

Stratospheric tracer modeling key aspects

B. Bregman et al.

Title Page

Abstract

Introduction

Conclusions

References

Tables

Figures

◀

▶

◀

▶

Back

Close

Full Screen / Esc

Printer-friendly Version

Interactive Discussion

modeling because of cloud processes, convection and other physical processes which are important for tracer transport. This is one of the major reasons why the majority of the current global models, including CTMs and CCMs use a fixed pressure or a hybrid sigma-pressure coordinate system, without implying that all these physical processes are accurately represented when using a hybrid sigma-pressure coordinate.

A fundamental question remains: are we able to perform meaningful multi-year tracer integrations applying DAS winds with a sigma-pressure vertical coordinate? The answer depends on the progress in improving DAS wind quality and the way they are applied in global models. Improving the quality of DAS winds is an ongoing activity and progress is being made in filtering techniques and the error covariances and bias corrections (Polavarapu et al., 2005), Simmons, personal communication). In this study we concentrate on how DAS winds are applied in CTMs.

One aspect not commonly addressed in CTM studies applying DAS winds is the effect of the update time interval on the modeled tracer distributions and the variability within the time interval. Generally the winds are updated every 6 h. However, stratospheric dynamical variability occurs on time scales shorter than 6 h (Shepherd et al., 2000; Manson et al., 2002), so that a considerable part of real variability is neglected. Additionally, the winds can be assumed constant over this time interval (instantaneous), averaged or interpolated in time. Instantaneous winds introduce discontinuities when changing time interval, leading to spurious variability, while averaging can be regarded as a (strong) wave filter. Examining ERA40 winds, Legras et al. (2005) show that decreasing the meteorological update time interval from 6 to 3 h reduces spurious motions considerably.

There have only been very few model studies addressing 3-hourly meteorological data in CTMs (Wild et al., 2003; Legras et al., 2005; Berthet et al., 2006). However, a more general evaluation at different spatial scales and including the effect of interpolation within the time interval has not yet been performed.

To evaluate all these key aspects for tracer transport we perform a variety of integrations, including different model grid resolutions and vertical layers, as well as different

Stratospheric tracer modeling key aspects

B. Bregman et al.

Title Page

Abstract

Introduction

Conclusions

References

Tables

Figures

◀

▶

◀

▶

Back

Close

Full Screen / Esc

Printer-friendly Version

Interactive Discussion

time intervals of the DAS winds, including time averaging and interpolation effects. We use CH₄ as a passive tracer to focus on polar transport in a similar set-up as in [van den Broek et al. \(2003\)](#). We further apply the age of air diagnose as a first-order approximation of the impact on the large-scale stratospheric meridional circulation and perform trajectory calculations to examine the degree of dispersion in the tropical lower stratosphere in the assimilated winds.

The outline of this paper is as follows. We first briefly describe TM5 and the recent updates. The next section addresses the model sensitivity experiments for the polar region, the general stratospheric circulation and dispersion in the tropical lower stratosphere, which is followed by a section describing the results. We will show that the model updates as well as the sensitivity experiments have a substantial impact on the tracer distributions. This section is followed by a summary of all comparisons providing guidelines for use of assimilated winds in CTMs.

2 Model description

The global Tracer Model, TM5 is a grid point Eulerian 3-D CTM and is an extended version of the TM3 model. The TM3 model has been used widely in the modeling community (e.g. [Dentener et al., 1999](#); [Peters et al., 2001](#); [Houweling et al., 1998](#); [Van den Broek et al., 2000](#); [Bregman et al., 2001, 2002](#)). The original version of the model has been developed by [Heimann \(1995\)](#); [Heimann and Keeling \(1989\)](#). TM5 uses forecasts of the European Centre for Medium-range Weather Forecasts (ECMWF) to drive the transport with a default update time interval of 6 h. It further uses mass fluxes for advection of the tracers as described in [van den Broek et al. \(2003\)](#). The model contains a Cartesian grid and consists of a two-way nested grid zooming over selected areas by increasing the horizontal resolution, currently up to 1°×1°. The model further contains hybrid σ -pressure levels with the top level at 0.1 hPa. The representation of the model winds has recently been adjusted to assure mass conservation by ([Segers et al., 2002](#)), which improved the representation of the model tracer fields significantly

Stratospheric tracer modeling key aspects

B. Bregman et al.

Title Page

Abstract

Introduction

Conclusions

References

Tables

Figures

◀

▶

◀

▶

Back

Close

Full Screen / Esc

Printer-friendly Version

Interactive Discussion

(Bregman et al., 2003).

An important feature of the TM5 zoom version is the mass consistent two-way nesting that allows global studies including zoom areas. Because of the grid zooming capability the model architecture has changed fundamentally. The model structure and the zooming concept have been described in detail and the model was successfully validated for the lower troposphere by Krol et al. (2005).

A validation of stratospheric tracers was performed by van den Broek et al. (2003). The TM5 version used in this study differs in some important aspects from the version used by van den Broek et al. In the previous version used by van den Broek et al. (2003), the advection scheme contained only first-order moments or slopes (Russel and Lerner, 1981). This version also uses second-order moments advection (Prather, 1986). Further, the previous version used a fixed number of vertical levels, while this version allows different vertical resolutions. Another important update is the ability to adjust the model advection time step locally when the CFL criterion (i.e., air mass transport exceeding the grid cell in one model advection time step) is violated (Krol et al., 2005). This update avoids a reduction of the polar grid in the polar regions, and thus allows a proper sensitivity study of model grid resolution.

The reduction of the polar grid is necessary because the horizontal grid cell area of a regular model grid decreases towards the poles and even becomes so small that the CFL criterium is violated and negative grid and consequently negative tracer mass would occur. This is particularly relevant for models containing mass-flux advection. To avoid this, without reducing the advection time step too severely, the model grid is artificially reduced. This reduction is established either by merging of the grid cells or the mass fluxes. See Sect. 2.3 in Krol et al. (2005) for a detailed description of the reduced grid treatment in TM5. In van den Broek et al. (2003) the reduced polar grid is illustrated within the zoom grid in Fig. 1 of that paper.

Up to now the reduction of the polar grid has not be validated because of computational limits, since the advection time steps would not only become excessively small (i.e. a few minutes only), but they would also have to be applied over the whole model

Stratospheric tracer modeling key aspects

B. Bregman et al.

Title Page

Abstract

Introduction

Conclusions

References

Tables

Figures

◀

▶

◀

▶

Back

Close

Full Screen / Esc

Printer-friendly Version

Interactive Discussion

domain. The new advection algorithm allows sufficiently small advection time steps by means of an iteration procedure for the location where a CFL isolation occurs, rather than by applying it over the whole grid. Whenever a CFL violation occurs, the number of iterations is determined by reducing the mass fluxes accordingly until the violation vanishes. Then the advection is performed with the required number of iterations. The iteration was tested for numerical errors by using idealized passive tracers, and the errors remained close to machine precision (not shown). This improvement was crucial, because it allows integrations at higher model grid resolutions.

3 Experimental set-up

For the model evaluation in the Arctic region methane was used as a passive tracer and the model was integrated from October 1999 to April 2000. The experimental setup, including the model constraints, are similar as in [van den Broek et al. \(2003\)](#). The reader is referred to this study for more details. We would like to emphasize that this experiment focuses on the high latitudes, since methane is treated as a passive tracer. For this reason the integration period is not more than half a year, but is sufficient for the purpose of this experiment. However, caution must be taken for mid-latitudes in the middle and upper stratosphere where the impact of chemistry becomes more pronounced.

The mean age of air is calculated by applying the “tracer pulse” method, as described in [Hall and Plumb \(1994\)](#) and [Hall et al. \(1999\)](#). The tracer pulse method consists of an inert tracer released in the troposphere with unity mass mixing ratio by applying a delta-function. The tracer mixing ratios in the stratosphere are a measure of the mean residence time, calculated using the Green function ([Hall and Plumb, 1994](#)). The year 2000 is integrated repetitively for 20 years. The mean age is calculated as the first moment of the derived spectrum after 20 years.

For the trajectory experiment the trajectory model is used as described by [Scheele et al. \(2005\)](#). Using the same experimental setup as in [Scheele et al. \(2005\)](#) we exam-

Stratospheric tracer modeling key aspects

B. Bregman et al.

Title Page

Abstract

Introduction

Conclusions

References

Tables

Figures

◀

▶

◀

▶

Back

Close

Full Screen / Esc

Printer-friendly Version

Interactive Discussion

ined the dispersion of air parcels in the tropical lower stratosphere by calculating 50-day back trajectories similar to the experiments performed by [Schoeberl et al. \(2002\)](#). Approximately 10000 trajectories started between 10° S–10° N at 460 K potential temperature level, corresponding to a pressure of 50 hPa or approximately 20 km altitude.

5 As a measure of dispersion, the fraction of air parcels crossing the 10° S and 10° N border before moving through the tropopause is calculated. Figure 1 shows the setup of the experiment. The tropopause is defined on basis of potential vorticity or temperature lapse rate. See [Scheele et al. \(2005\)](#) for a detailed discussion. In addition to the meteorology used by the CTM, we have applied ERA40 forecasts.

10 The default setup of TM5 includes a global horizontal resolution of $3 \times 2^\circ$, 45 vertical layers and a second-order moment advection scheme, no reduction of the polar grid resolution and using instantaneous (constant) wind fields updated every 6 h. In addition, a zoom grid with a horizontal resolution of $1 \times 1^\circ$ was applied between 30°–90° N, similar as in [van den Broek et al. \(2003\)](#) (see their Fig. 1). All 60 layers of the ECWMF fields have been used, and two subsets with fewer layers: (i) 45 layers, containing all stratospheric and upper tropospheric levels and a reduced number only in the lower troposphere, and (ii) 30 layers, which are obtained by subtracting every second layer from the 60-layer fields. The default number of vertical layers is 45. The results with 45 layers are similar to those using 60-layers (not shown). Two advection schemes were used, a first-order “slopes” scheme ([Russel and Lerner, 1981](#)) and a second-order moments scheme ([Prather, 1986](#)), with the slopes scheme being most diffusive. Note that with the current model configuration, integrations including a zoom area could only be performed with the first-order advection scheme. The effect of the reduced polar grid was examined in all model configurations. Additional experiments were performed to examine the time discretization. Using the default model setup we used 3-hourly instead of 6-hourly meteorological data. We further interpolated the winds in time within the update time intervals for both the 6-hourly and the 3-hourly setup to investigate the effect of including wind variability within the meteorological update time interval. The default setup is using 6-hourly instantaneous winds.

Stratospheric tracer modeling key aspectsB. Bregman et al.

Title Page

Abstract

Introduction

Conclusions

References

Tables

Figures

◀

▶

◀

▶

Back

Close

Full Screen / Esc

Printer-friendly Version

Interactive Discussion

A summary of the sensitivity experiments is given in Table 1. Changes to this set are mentioned explicitly in the text.

4 Results

4.1 Horizontal cross sections in the polar region

5 Horizontal cross sections of CH₄ at 35 hPa have been made for 15 March 2000, after integrating the model through the 1999/2000 Arctic winter for five different model versions. This day has been chosen for various reasons. The vortex was still very strong at this stage of the winter so that potential model deficits would be discernible more clearly after accumulation over the whole winter, as was demonstrated in previous model intercomparison (van den Broek et al., 2003). In addition, the late winter vortex becomes subject of considerable dynamic disturbances, providing a useful test for CTMs to capture the dynamic features.

15 Figure 2 shows the results for the “default”, “red grid”, “1×1” runs with all 6-hourly instantaneous or constant winds, and for the runs with 6-hourly and 3-hourly interpolated winds. The methane levels from the reduced grid run are clearly higher with a very weak vortex edge and little tracer variability compared to the fields from the other runs. The “default” and the “1×1” runs yield much stronger vortex edges and more variability and both fields are quite comparable. The vortex edge tracer gradients will be shown in more detail in Figs. 7 and 8. The vortex gradients become slightly stronger when using the 6-hourly interpolated wind, and considerably stronger when using 3-hourly interpolated winds. Also outside the vortex the tracer fields are considerably lower in this model version, indicating that applying time interpolation and in particular increasing the update frequency affects the tracer distribution on a large (hemispheric) scale. Berthet et al. (2006) also shows reduction in N₂O, HNO₃ and NO₂ in the mid-latitude middle stratosphere when applying 3-hourly winds.

25 We now will compare the modeled CH₄ fields in more detail by comparing the results

Stratospheric tracer modeling key aspects

B. Bregman et al.

Title Page

Abstract

Introduction

Conclusions

References

Tables

Figures

◀

▶

◀

▶

Back

Close

Full Screen / Esc

Printer-friendly Version

Interactive Discussion

with balloon- and space-borne vertical profiles inside the polar vortex and with space-borne observations across the vortex edge.

4.2 Comparison with balloon-borne profiles inside the polar vortex

We show a series of figures with comparisons of calculated and observed CH₄ profiles for all different model versions. The observations consist of balloon- and space-borne profiles sampled in the polar vortex from December 1999 to April 2000. The selected balloon profiles were all inside the polar vortex and in the study of [van den Broek et al. \(2003\)](#) the largest model underestimation was found for these profiles. The observations were obtained from the balloon-borne Tunable Diode Laser Absorption Spectrometer (TDLAS) ([Garcelon et al., 2002](#)), the Jet Propulsion Laboratory MkIV interferometer ([Toon et al., 1999](#)), and the space-borne HALogen Occultation Experiment (HALOE) ([Russel-III et al., 1993](#)) on board the UARS satellite. The balloon-borne observations were performed in the frame of the combined projects THird European Stratospheric Experiment on Ozone (THESEO) and Sage III Ozone Loss and Validation Experiment (SOLVE). See [van den Broek et al. \(2003\)](#) for more details.

Figure 3 shows a comparison with observations for the model versions “default”, “red. grid”, “slopes”, and “30L”. In December the model results are close to the observations. However, the model overestimates CH₄ later in the winter and the overestimation increases in time. Note that the “slopes” results are similar to those presented in [van den Broek et al. \(2003\)](#) and considerably overestimates the observed CH₄ profiles. Another feature is the significant improvement when applying less diffusive second-order moments advection. However, the model still overestimates the tracer concentrations. The results from the “red. grid” run are similar to the “slopes” run, but are performed with the second-order moments advection scheme, and reflects the effect of the reduced polar grid. This quite dramatic effect is also visible in Fig. 2. This result is quite remarkable, since the reduced grid extends to 70° N only, while the balloon profiles were located more southwards.

The improvement when removing the reduced polar grid gives an important mes-

Stratospheric tracer modeling key aspects

B. Bregman et al.

Title Page

Abstract

Introduction

Conclusions

References

Tables

Figures

◀

▶

◀

▶

Back

Close

Full Screen / Esc

Printer-friendly Version

Interactive Discussion

sage to those who apply some kind of grid or mass flux or wind vector merging in the polar region. Another important effect is that a reduction of the polar grid obscures evaluation of grid resolution. To demonstrate this we applied the diffusive first-order slopes advection, as was done in [van den Broek et al. \(2003\)](#) but now with model grid zooming up to the pole (run “1×1”). Figure 4 shows that the results improved significantly and are comparable or occasionally even slightly better than the results from the default run with second-order moments advection. This is in contrast with the previous evaluation in [van den Broek et al. \(2003\)](#) where grid zooming did not improve the results and clearly demonstrate the danger of polar grid reduction.

The significant improvement in tracer distribution when increasing the horizontal resolution from 3°×2° to 1°×1° illustrates that model grid resolution is a key issue for the diffusivity of advection. The “1×1” run used the relatively diffusive first-order slopes advection scheme, while the “default” run used much less diffusive second-order moments advection.

The numerical diffusion depends on the amount of tracer information for a given grid cell volume. Figure 6 shows the tracer information for a 3°×2° grid cell in the case of the “default” run (left panel), the “slopes” run (middle panel) and the “1×1” run (right panel). The “default” run contains 10 parameters that determine the tracer level: the first-order slopes (3), the second-order moments (6), and the tracer mass (1). In contrast, the “slopes” run only contains 4 variables with tracer information: the first-order slopes (3) and the tracer mass (1). On the other hand, the zoom region contains 6 more grid cells with each 4 tracer parameters, resulting in a total of 24. The “slopes” run contains the least amount of tracer information and clearly yields the worst results. However, the amount of tracer information in the “1×1” run is twice more than that of the “default” configuration for a 3°×2° grid cell, but shows no improvement in the tracer distribution. This may indicate a resolution threshold, which support the findings by [Searle et al. \(1998\)](#). However, this study demonstrates that such a threshold, if present, depends on the way tracer advection is performed. A diffusive advection scheme clearly overrules the advantage of resolution increase, at least up to 1°×1°. It will also depend on the

Stratospheric tracer modeling key aspectsB. Bregman et al.

Title Page

Abstract

Introduction

Conclusions

References

Tables

Figures

◀

▶

◀

▶

Back

Close

Full Screen / Esc

Printer-friendly Version

Interactive Discussion

chemical lifetime of the tracer in question and for a species such as ClO the impact of resolution increase may be substantial (Marchand et al., 2003; Tan et al., 1998).

Next a sensitivity test of vertical resolution was performed. By comparing “default” with “30L” Fig. 3 shows that the effect of doubling the vertical resolution is restricted to the upper stratosphere (i.e., above the 10 hPa pressure level) where both profiles start to deviate. Due to the limited altitude range of the balloon, no detailed comparison could be performed in the upper stratosphere. Nevertheless, these results indicate that for the current model configuration and experimental setup, vertical resolution does have a significant impact on the tracer distribution, but only in the upper stratosphere.

Finally, we examined the effect of using more wind variability as given by the assimilated wind fields. Figure 5 shows the calculated CH₄ profiles from the “default” run, i.e., with instantaneous 6-hourly wind fields, similar as in Fig. 3 and 6. By interpolating the winds between two subsequent time intervals we account for the wind variability within the model integration time interval. The agreement with observations improves, especially on 15 March 2000. Applying 3-hourly interpolated winds the results are in excellent agreement with the observations.

These results demonstrate the importance to avoid constant winds within the meteorological time interval and in particular the importance of the update frequency of the DAS winds, which was also shown for mid-latitude tracer profiles in Berthet et al. (2006). Apparently, more real variability is introduced when applying 3-hourly instead of 6-hourly winds, rather than more “noise”.

4.3 Comparison with satellite observations: tracer gradient across the vortex edge

Next, we focus on the tracer gradient through the vortex edge. A comparison is performed with 15 profiles observed by the HALOE instrument on board the UARS satellite. See van den Broek et al. (2003) for a more detailed description of these observations. These profiles were part of the HALOE sweeps close to the edge of the polar vortex, covering both mid-litudinal extra- and polar vortex air, and are thus very suitable to focus on the vortex edge. For such a comparison an equivalent, instead of the

Stratospheric tracer modeling key aspects

B. Bregman et al.

Title Page

Abstract

Introduction

Conclusions

References

Tables

Figures

◀

▶

◀

▶

Back

Close

Full Screen / Esc

Printer-friendly Version

Interactive Discussion

regular Cartesian, latitude coordinate is more useful. Three different potential temperature levels have been selected, one close to the polar vortex bottom (425 K), one in the lower stratosphere (500 K) and one in the middle stratosphere (600 K).

Figures 7, 8 and 9 show the results of this comparison for the “default”, “red. grid”, “1 × 1” runs, “6-hourly-interp” and “3-hourly-interp” experiments. The comparisons are somewhat obscured by the relatively large scatter in the observations, the limited coverage in the polar vortex and the modeled variability (denoted by the vertical bar as 1σ). The scatter in the observations is most probably due to the differences in the sampling volume of the observations and the ECWMF potential temperature and potential vorticity grid cell volumes. Nevertheless, the latitudinal coverage is sufficient and the tracer gradient across the vortex edge is clearly discernible. As expected, the gradient becomes more pronounced with increasing potential temperature level, both in the observations and in the model results. The default run agrees quite reasonable, while significant underestimation is found for the “red. grid” run, in line with the findings in Fig. 3. The tracer gradient at the vortex edge is manifested most clearly in the “1 × 1” run, although the overall gradient is similar to the default run.

It is interesting that the modeled variability is significantly reduced in the zoom region, especially in active mixing regions: close to the vortex bottom and at the vortex edge. This reflects the increased tracer information in the zoom region, despite the more diffusive advection scheme (see Fig. 6).

Figure 7 indicates that the impact of the reduced grid exceeds the polar region. The southern border of the reduced grid in the Arctic is 70° N, but the differences with the default run extends to 60° N equivalent latitude. It is remarkable that the impact is found even further south in instantaneous fields. As was demonstrated in Fig. 8 the differences with the zoom region are small with differences up to about 10% and arise at locations where vortex filaments are present.

As can be seen in Fig. 9 the calculated gradients became stronger when introducing time interpolation and in particular by increasing the meteorological update frequency, in line with the model results described earlier. The differences with the results from the

Stratospheric tracer modeling key aspectsB. Bregman et al.

[Title Page](#)[Abstract](#)[Introduction](#)[Conclusions](#)[References](#)[Tables](#)[Figures](#)[◀](#)[▶](#)[◀](#)[▶](#)[Back](#)[Close](#)[Full Screen / Esc](#)[Printer-friendly Version](#)[Interactive Discussion](#)

default run increase with increasing potential temperature level. At 600 K the model underestimates the observations at 50–60° N outside the polar vortex, which is apparent in the results from all model experiments.

Note that even in the best model performance the calculated gradient is slightly underestimated, indicating remaining diffusivity and/or the lack of chemistry. Although the effect of chemistry has been tested to have a negligible impact on methane at levels below 10 hPa in a similar model experiment (van Aalst et al., 2004), caution must be taken by treating methane as a passive tracer. Especially close to more chemically active regions of the atmosphere, i.e., the upper stratosphere outside the polar vortex. Indicative for this influence could be the slight underestimation by the model in Figs. 8 and 9 at the highest potential temperature level (600 K), which is not present at lower potential temperature levels.

4.4 Age of air experiment

In this experiment we focus on the large-scale meridional circulation in the stratosphere by calculating the mean age of air, as described in the section experimental setup. Here we examine if the earlier found disagreements in calculated and observed mean age of air (Meijer et al., 2004) can be improved by applying 3-hourly DAS winds and time interpolation. We also omitted the reduced polar grid. For the evaluation of the modeled mean age of air we use a compilation of CO₂ and SF₆ observed on board the ER-2 between 1991–1998 (Andrews et al., 2001), as in Meijer et al. (2004).

Figure 10 shows the calculated zonally average mean age of air for three different runs using 6-hourly instantaneous (top panel), 6-hourly interpolated (middle panel) and 3-hourly interpolated winds (bottom panel). The mean age of air is significantly older when using 3-hourly instead of 6-hourly interpolated winds. The effect of interpolation is less significant, although the air becomes 0.5 year older in the upper stratosphere when applying time interpolating in the 6-hourly winds.

Figure 11 shows the calculated zonally average mean age of air for the same three runs, but now at approximately 20 km altitude, compared to observations. The obser-

Stratospheric tracer modeling key aspects

B. Bregman et al.

Title Page

Abstract

Introduction

Conclusions

References

Tables

Figures

◀

▶

◀

▶

Back

Close

Full Screen / Esc

Printer-friendly Version

Interactive Discussion

5 vations represent mean age of air derived from airborne in-situ CO₂ measurements on board the ER-2 aircraft in the lower stratosphere (Andrews et al., 2001). The measurements are a compilation of all observations between 1991 and 1998. In line with Fig. 10 the use of 3-hourly interpolated winds gives the oldest mean age of air. Note that the meridional gradient is significantly steeper than using 6-hourly winds, indicative of reduced dispersion. Nevertheless the calculated mean age still remains about one year too young in the extra-tropical lower stratosphere. Applying time interpolation in the 6-hourly winds only yields a small improvement. As shown in Fig. 10 the effect of time interpolation is discernible mainly in the middle and upper stratosphere.

10 The mean age of air from the 6-hourly instantaneous winds is similar to that calculated by Meijer et al. (2004), although they applied a reduced polar grid. This indicates that, in contrast to the findings in the polar study, the reduced polar grid does not affect the stratospheric large-scale tracer transport.

4.5 Back-trajectory experiments

15 Next we focus on the tropical lower stratosphere, since it is a key region for the large-scale meridional circulation. With back-trajectory calculations we calculate the dispersion of air parcels over 50 days. This time scale is much shorter than the mean age of air, but the dispersion intensity is a useful measure of the noise in DAS winds and thus indirectly relates to the mean age of air (Schoeberl et al., 2002; Scheele et al., 2005). In these calculations we only used interpolated winds. So far we have examined the effect of increasing the update frequency with 4DVAR OD data only. It is interesting to investigate the effect using 3DVAR ERA40 data. We therefore examined three different DAS winds: (1) the default OD 6-hourly winds (red line), similar to the results in Fig. 2 in Scheele et al. (2005). The second and third data set is derived from the 3DVAR ERA40 6-hourly and 3-hourly winds, respectively. Figure 12 shows the end points of the air parcels after 50 days. There is considerable scatter, similar to the results from Schoeberl et al. (2002). As expected, the 6-hourly winds from OD are less dispersive than those from ERA40, as already discussed by Scheele et al. (2005). However, the

Stratospheric tracer modeling key aspects

B. Bregman et al.

Title Page

Abstract

Introduction

Conclusions

References

Tables

Figures

◀

▶

◀

▶

Back

Close

Full Screen / Esc

Printer-friendly Version

Interactive Discussion

3-hourly winds from ERA40 show much less vertical dispersion, even compared to the generally less noisy OD winds. Interestingly, the horizontal dispersion is not reduced in the 3-hourly winds.

Figure 13 shows the fraction of air parcels leaving the 10° S–10° N latitude band before crossing the tropopause as a measure of dispersion versus the integration time (50 days). In line with Fig. 12, the 3DVAR winds (ERA40 6-hourly) show a significant large fraction than the 4DVAR winds (OD 6-hourly). This result is similar as in Scheele et al. (2005). Adding the 3-hourly ERA40 data results in a strong decrease of the fraction. It is even smaller than that calculated with the 6-hourly OD using 4DVAR assimilation.

5 Conclusions

In this study we used a CTM (TM5) to investigate the impact of a variety of different model configurations and different representations of the assimilated meteorology on stratospheric tracer transport. In particular we examined the impact of model grid resolution, including the reduction of the polar grid, the diffusivity of the advection scheme, and the update frequency and variability in DAS winds. As a diagnose we used CH₄ transport in the Arctic polar vortex and the mean age of air. We further applied a trajectory model to investigate air parcel dispersion in the tropical lower stratosphere.

This study shows that the commonly applied artificial reduction of the polar grid of wind field averaging does have a significant impact on the tracer distribution. The impact well exceeds the area of the reduced grid and these results contain an important message for other studies on polar tracer transport with global models.

The sensitivity experiments show that doubling the vertical resolution substantially affects the tracer distribution in the upper stratosphere, i.e., above 10 hPa, but not below this pressure level. The model results in the upper stratosphere can unfortunately not be evaluated due to a lack of observations.

On the course of a winter increasing the horizontal resolution to 1° × 1° improves the

Stratospheric tracer modeling key aspects

B. Bregman et al.

Title Page

Abstract

Introduction

Conclusions

References

Tables

Figures

◀

▶

◀

▶

Back

Close

Full Screen / Esc

Printer-friendly Version

Interactive Discussion

CH₄ distribution in the polar vortex considerably when using first-order (slopes) advection. This is to be expected, since a higher grid resolution represents the vortex edge more realistically. Note that this is only valid without a reduced polar grid. These results are an update of a previous model study where an increase in horizontal grid resolution did not improve the tracer distributions using the same experimental setup. This contrasting result clearly demonstrates the danger of using a reduced polar grid when evaluating model grid resolution. By using adjustable advection time steps, proper high resolution global modeling is feasible in the polar regions.

The impact on stratospheric CH₄ distribution in the polar region by applying more wind variability in the CTM integrations is significant. Using 6-hourly time interpolated instead of instantaneous winds resulted in reduced cross vortex edge mixing and closer agreement with the observed CH₄ profiles inside the vortex. Reducing the time interval to 3 h improves the model results even further and yielded excellent agreement with the observed CH₄ profiles inside the Arctic vortex.

The stratospheric meridional circulation is examined by diagnosing the mean residence time of air in the stratosphere (mean age of air). The mean age of air becomes significantly older in the extra-tropical stratosphere when applying 3-hourly instead of 6-hourly interpolated winds. This indicates that introducing more variability in the wind fields reduces the dispersion. The use of time interpolation is particularly noticeable in the middle and upper stratosphere where the mean age of air becomes 0.5 year older. The tropical mean age of air shows excellent agreement with observations, although the extra-tropical lower stratospheric mean age remains too young with about one year.

According to the back-trajectory calculations, the use of 3-hourly winds leads to less vertical dispersion, even with winds produced by the more noisy ERA40 re-analyses winds. It is important to note that the use of 3-hourly winds does not introduce more noise, but more real variability in the wind fields. It remains to be determined what is the most suitable update frequency for stratospheric tracer transport. Such a question is directly related to the representation of the winds from the GCM that provides the winds to the data assimilation system. [Vaughn et al. \(1997\)](#) discussed different time

Stratospheric tracer modeling key aspects

B. Bregman et al.

Title Page

Abstract

Introduction

Conclusions

References

Tables

Figures

◀

▶

◀

▶

Back

Close

Full Screen / Esc

Printer-friendly Version

Interactive Discussion

intervals and averaging, however, not for time frequencies of 3 or even less hours. Investigating this problem is however not trivial and is subject of further study.

For models using vertical hybrid sigma-pressure coordinates recent new insights in the use of DAS winds in CTMs has improved the stratospheric tracer representation considerably, both in the polar region as on the large scale. It is recommended not to use a reduction of the polar grid (either through grid cell merging or by wind averaging). We also recommend to apply time interpolation instead of using instantaneous winds. In line with the findings from [Legras et al. \(2005\)](#) it is also recommended to apply 3-hourly instead of the commonly used 6-hourly update interval. These results in combination with improvements in data assimilation procedures give new perspectives for long-term tracer integrations.

Acknowledgements. Part of this work is funded by the European Commission, through the project TOwards the Prediction of stratospheric OZone (TOPOZ) III, under contract no. EVK2-CT-2001-00102, the project Stratospheric-Climate Links with Emphasis on the Upper Troposphere and Lower Stratosphere (SCOUT), and the National (Netherlands) User Support Programme (GO)2. We thank M. Krol and A. Segers for computational support and useful discussions.

References

- Andrews, A., Boering, K., Daube, B., Wofsy, S., Loewenstein, M., Jost, H., Podolske, J., Webster, C., Herman, R., Scott, D., Flesh, G., Moyer, E., Elkins, J., Dutton, G., Hurst, D., Moore, F., Ray, E., Romanschkin, P., and Strahan, S.: Mean ages of stratospheric air derived from in situ observations of CO₂, CH₄, and N₂O, *J. Geophys. Res.*, 106, 32 295–32 314, 2001. [4391](#), [4392](#), [4412](#)
- Berthet, G., Huret, N., Lefèvre, F., Moreau, G., Robert, C., Chartier, M., Pomathiod, L., Pirre, M., and Catoire, V.: On the ability of chemical transport models to simulate the vertical structure of the N₂O, NO₂ and HNO₃ species in the mid-latitude stratosphere, *Atmos. Chem. Phys.*, 6, 1599–1609, 2006. [4381](#), [4386](#), [4389](#)

Stratospheric tracer modeling key aspects

B. Bregman et al.

Title Page

Abstract

Introduction

Conclusions

References

Tables

Figures

◀

▶

◀

▶

Back

Close

Full Screen / Esc

Printer-friendly Version

Interactive Discussion

Stratospheric tracer modeling key aspects

B. Bregman et al.

Title Page

Abstract

Introduction

Conclusions

References

Tables

Figures

◀

▶

◀

▶

Back

Close

Full Screen / Esc

Printer-friendly Version

Interactive Discussion

Bregman, A., Krol, M., Teyssède, H., Norton, W., Chipperfield, M., Pitari, G., Sundet, J., and Lelieveld, J.: Chemistry-transport model comparison with ozone observations in the midlatitude lowermost stratosphere, *J. Geophys. Res.*, 106, 17 479–17 496, 2001. [4382](#)

Bregman, A., Wang, P.-H., and Lelieveld, J.: Chemical ozone loss in the tropopause region on subvisible ice clouds, calculated with a chemistry-transport model, *J. Geophys. Res.*, 107, doi:10.1029/2001JD000761, 2002. [4382](#)

Bregman, B., Segers, A., Krol, M., Meijer, E., and van Velthoven, P.: On the use of mass-conserving wind fields in chemistry-transport models, *Atmos. Chem. Phys.*, 3, 447–457, 2003. [4380](#), [4383](#)

Chipperfield, M.: New version of the TOMCAT/SLIMCAT off-line chemical transport model: Intercomparison of stratospheric tracer experiments, *Q. J. R. Meteorol. Soc.*, in press, 2006. [4379](#), [4380](#)

Dentener, F., Feichter, J., and Jeuken, A.: Simulation of the transport of Rn^{222} using on-line and off-line global models at different horizontal resolutions: A detailed comparison with measurements, *Tellus*, 51, 573–602, 1999. [4382](#)

Douglass, A., Schoeberl, M. R., Rood, R. B., and Pawson, S.: Evaluation of transport in the lower tropical stratosphere in a global chemistry and transport model, *J. Geophys. Res.*, 108, 4259, doi:10.1029/2002JD002696, 2003. [4378](#)

Garcelon, S., Gardiner, T., Hansford, G., Harris, N., Howieson, I., Jones, R., McIntyre, J., Pyle, J., Robinson, J., Swann, N., and Woods, P.: Investigation of CH_4 and CFC-11 vertical profiles in the Arctic vortex during the SOLVE/THESEO 2000 campaign, in: Proceedings of the general Assembly, Nice, European Geophysical Society, 2002. [4387](#)

Hadjinicolaou, P., Pyle, J. A., and Harris, N. R. P.: The recent turnaround in stratospheric ozone over northern middle latitudes: A dynamical modeling perspective, *Geophys. Res. Lett.*, 32, L12821, doi:10.1029/2005GL022476, 2005. [4379](#)

Hall, T. and Plumb, R.: Age as a diagnostic of stratospheric transport, *J. Geophys. Res.*, 99, 1059–1070, 1994. [4384](#)

Hall, T., Waugh, D., Boering, K., and Plumb, R.: Evaluation of transport in stratospheric models, *J. Geophys. Res.*, 104, 18 815–18 839, 1999. [4384](#)

Heimann, M.: The Global Atmospheric Tracer Model TM2, Tech. Rep. 10, DRKZ-Hamburg, 1995. [4382](#)

Heimann, M. and Keeling, C.: A three-dimensional model of atmospheric CO_2 transport based on observed winds: 2: Model description and simulated tracer experiments, *Geophys. Mon.*,

55, 237–275, 1989. [4382](#)

Houweling, S., Dentener, F., and Lelieveld, J.: The impact of non-methane hydrocarbon compounds on tropospheric photochemistry, *J. Geophys. Res.*, 103, 10 673–10 696, 1998. [4382](#)

Jöckel, P., von Kuhlmann, R., Lawrence, M., Steil, B., Brenninkmeijer, C., Crutzen, P., Rasch, P., and Eaton, B.: On a fundamental problem in implementing flux-form advection schemes for tracer transport in 3-dimensional general circulation and chemistry transport models, *Q. J. R. Meteorol. Soc.*, 127, 1035–1052, 2001. [4380](#)

Krol, M., Houweling, S., Bregman, B., van den Broek, M., Segers, A., van Velthoven, P., Peters, W., Dentener, F., and Bergamaschi, P.: TM5, a global two-way nested chemistry transport zoom model: algorithm and applications, *Atmos. Chem. Phys.*, 5, 417–432, 2005. [4378](#), [4383](#)

Laat, A., Landgraf, J., Aben, I., Hasekamp, O., and Bregman, B.: Assimilated winds for global modelling: evaluation with space- and balloon-borne ozone observations, *J. Geophys. Res.*, in press, 2006. [4379](#)

Legras, B., Pissot, I., Berthet, G., and Lefèvre, F.: Variability of the Lagrangian turbulent diffusion in the lower stratosphere, *Atmos. Chem. Phys.*, 5, 1605–1622, 2005. [4381](#), [4395](#)

Mahowald, N. M., Plumb, R. A., Rasch, P. J., del Corral, J., Sassi, F., and Heres, W.: Stratospheric transport in a three-dimensional isentropic coordinate model, *J. Geophys. Res.*, 107(D15), 4254, doi:10.1029/2001JD001313, 2002. [4380](#)

Manney, G., Allen, D., Krüger, K., Naujokat, B., Santee, M., Sabutis, J., Pawson, S., Swinbank, R., Randall, C., Simmons, A. J., and Long, G.: Diagnostic comparison of meteorological analyses during the 2002 Antarctic winter, *J. Atmos. Sci.*, 133, 1261–1278, 2005. [4379](#)

Manson, A., Meek, C., Koshyk, J., Franke, S., Fritts, D., Riggan, D., Hall, C., Hocking, W., MacDougall, J., Igarashi, K., and Vincent, R.: Gravity wave activity and dynamical effects in the middle atmosphere (60–90 km): observations from an MF/MLT radar network, and results from the Canadian Middle Atmosphere Model (CMAM), *J. Atmos. Solar-Terr. Phys.*, 64, 65–90, 2002. [4381](#)

Marchand, M., Godin, S., Hauchecorne, A., Lefèvre, F., and Chipperfield, M.: Influence of polar ozone loss on northern midlatitude regions estimated by a high-resolution chemistry transport model during winter 1999/2000, *J. Geophys. Res.*, 108, 8326, doi:10.1029/2001JD000906, 2003. [4377](#), [4389](#)

Meijer, E. W., Bregman, B., Segers, A., and van Velthoven, P. F. J.: The influence of data assimilation on the age of air calculated with a global chemistry-transport model using ECMWF

ACPD

6, 4375–4414, 2006

Stratospheric tracer modeling key aspects

B. Bregman et al.

Title Page

Abstract

Introduction

Conclusions

References

Tables

Figures

◀

▶

◀

▶

Back

Close

Full Screen / Esc

Printer-friendly Version

Interactive Discussion

EGU

winds, *Geophys. Res. Lett.*, 31, L23114, doi:10.1029/2004GL021158, 2004. [4378](#), [4379](#), [4380](#), [4391](#), [4392](#)

Peters, W., Krol, M. C., Dentener, F. J., and Lelieveld, J.: Identification of an El Niño-Southern Oscillation signal in a multiyear global simulation of tropospheric ozone, *J. Geophys. Res.*, 106, 10 389–10 402, 2001. [4382](#)

Polavarapu, S., Ren, S., Rochon, Y., Sankey, D., Ek, N., Koshyk, J., and Tarasick, D.: Data assimilation with the Canadian Middle Atmosphere Model, *Appl. Opt.*, 43, 77–100, 2005. [4381](#)

Prather, M.: Numerical advection by conservation of second-order moments, *J. Geophys. Res.*, 91, 6671–6681, 1986. [4383](#), [4385](#)

Randel, W., Fleming, E., Geller, M., Gelman, M., Hamilton, K., Karoly, D., Ortland, D., Pawson, S., Swinbank, R., Udelhofen, P., Wu, F., Baldwin, M., Chanin, M.-L., Keckhut, P., Simmons, A., and Wu, D.: The SPARC intercomparison of Middle Atmosphere Climatologies, *Tech. Rep. 20*, SPARC newsletter, 2003. [4379](#)

Rotman, D., Atherton, C., Bergmann, D., Cameron-Smith, P., Chuang, C., Connell, P., Dignon, J., Franz, A., Grant, K., Kinnison, D., Molenkamp, C., Proctor, D., and Tannahill, J.: IMPACT, the LLNL 3-D global atmospheric chemical transport model for the combined troposphere and stratosphere: Model description and analysis of ozone and other trace gases, *J. Geophys. Res.*, 109, D04303, doi:10.1029/2002JD003155, 2004. [4380](#)

Russel, G. and Lerner, J.: A new finite-differencing scheme for the tracer transport equation, *J. Appl. Meteorol.*, 20, 1483–1498, 1981. [4383](#), [4385](#)

Russel-III, J., Gordley, L., Park, J., Drayson, S., Hesketh, D., Cicerone, R., Tuck, A., Frederick, J., Harries, J., and Crutzen, P.: The Halogen Occultation Experiment, *J. Geophys. Res.*, 98, 10 777–10 797, 1993. [4387](#)

Scheele, R., Siegmund, P., and van Velthoven, P.: Stratospheric age of air computed with trajectories based on various 3-D-Var and 4-D-Var data sets, *Atmos. Chem. Phys.*, 5, 1–7, 2005. [4378](#), [4379](#), [4380](#), [4384](#), [4385](#), [4392](#), [4393](#)

Schoeberl, M., Douglass, A., Zhu, Z., and Pawson, S.: A comparison of the lower stratospheric age-spectra, derived from a General Circulation Model and two data assimilation systems., *J. Geophys. Res.*, 108, 4113, doi:10.1029/2002JD002652, 2002. [4378](#), [4385](#), [4392](#)

Searle, K., Chipperfield, M., Bekkie, S., and Pyle, J.: The impact of spatial averaging on calculated polar ozone loss, 1, Model experiments, *J. Geophys. Res.*, 103, 25 397–25 408, 1998. [4377](#), [4388](#)

Stratospheric tracer modeling key aspects

B. Bregman et al.

Title Page

Abstract

Introduction

Conclusions

References

Tables

Figures

◀

▶

◀

▶

Back

Close

Full Screen / Esc

Printer-friendly Version

Interactive Discussion

Stratospheric tracer modeling key aspects

B. Bregman et al.

Title Page

Abstract

Introduction

Conclusions

References

Tables

Figures

◀

▶

◀

▶

Back

Close

Full Screen / Esc

Printer-friendly Version

Interactive Discussion

- Segers, A., van Velthoven, P., Bregman, B., and Krol, M.: On the computation of mass fluxes for Eulerian transport models from spectral meteorological fields, in: Proceedings of the 2002 International Conference on Computational Science, Lecture Notes in Computer Science (LNCS), Springer Verlag, 2002. [4380](#), [4382](#)
- 5 Shepherd, T., Koshyk, J., and Ngan, K.: On the nature of large-scale mixing in the stratosphere and mesosphere, *J. Geophys. Res.*, 105, 12 433–12 446, 2000. [4381](#)
- Simmons, A., Hortal, M., Kelly, G., McNally, A., Untch, A., and Uppala, S.: ECMWF analyses and forecasts of stratospheric winter polar vortex breakup: September 2002 in the Southern Hemisphere and related events, *J. Atmos. Sci.*, 62, 668–689, 2005. [4379](#)
- 10 Tan, D., Haynes, P. H., MacKenzie, A. R., and Pyle, J. A.: Effects of fluid-dynamical stirring and mixing on the deactivation of stratospheric chlorine, *J. Geophys. Res.*, 103, 1585–1606, 1998. [4389](#)
- Toon, G., Blavier, J.-F., Sen, B., Margitan, J., Webster, C., May, R., Fahey, D., Gao, R., Negro, L. D., Proffit, M., Elkins, J., Romashkin, P., Hurst, D., Oltmans, S., Atlas, E., Schauffler, S., Flocke, F., Bui, T., Stimpfle, R., Boone, G., Voss, P., and Cohen, R.: Comparison of MkIV balloon and ER-2 aircraft measurements of atmospheric trace gases, *J. Geophys. Res.*, 104, 26 779–26 790, 1999. [4387](#)
- 15 van Aalst, M., van den Broek, M., Bregman, A., Brühl, C., Steil, B., Toon, G., Garcelon, S., Hansford, G., Jones, R., Gardiner, T., Roelofs, G., Lelieveld, J., and Crutzen, P.: Tracer transport in the 1999/2000 Arctic polar vortex comparison of nudged GCM runs with observations, *Atmos. Chem. Phys.*, 4, 81–93, 2004. [4391](#)
- Van den Broek, M., Bregman, A., and Lelieveld, J.: Model study of stratospheric chlorine and ozone loss during the 1996/1997 winter, *J. Geophys. Res.*, 105, 28 961–28 977, 2000. [4382](#)
- van den Broek, M., van Aalst, M., Bregman, A., Krol, M., Lelieveld, J., Toon, G., Garcelon, S., Hansford, G., Jones, R., and Gardiner, T.: The impact of model grid zooming on tracer transport in the 1999/2000 Arctic polar vortex, *Atmos. Chem. Phys.*, 3, 1833–1847, 2003. [4377](#), [4382](#), [4383](#), [4384](#), [4385](#), [4386](#), [4387](#), [4388](#), [4389](#)
- 25 van Noije, T. P. C., Eskes, H. J., van Weele, M., and van Velthoven, P. F. J.: Implications of the enhanced Brewer-Dobson circulation in European Centre for Medium-Range Weather Forecasts reanalysis ERA-40 for the stratosphere-troposphere exchange of ozone in global chemistry transport models, *J. Geophys. Res.*, 109, D19308, doi:10.1029/2004JD004586, 2004. [4379](#)
- 30 Waugh, D. W., Hall, T. M., Randel, W. J., Rasch, P. J., Boville, B. A., Boering, K. A., Wofsy, S. C.,

Daube, B. C., Elkins, J. W., Fahey, D. W., Dutton, G. S., and Volk, C. M.: Three-dimensional simulations of long-lived tracers using winds from MACCM2, *J. Geophys. Res.*, 102(D17), 21 493–21 514, 1997. [4394](#)

5 Wild, O., Sundet, J. K., Prather, M. J., Isaksen, I. S. A., Akimoto, H., Browell, E. V., and Oltmans, S. J.: Chemical transport model ozone simulations for spring 2001 over the western Pacific: Comparisons with TRACE-P lidar, ozonesondes and Total Ozone Mapping Spectrometer columns, *J. Geophys. Res.*, 108(D21), 8826, doi:10.1029/2002JD003283, 2003. [4381](#)

WMO: Scientific Assessment of Ozone Depletion, Tech. Rep. 47, WMO, 2002. [4377](#)

ACPD

6, 4375–4414, 2006

Stratospheric tracer modeling key aspects

B. Bregman et al.

Title Page

Abstract

Introduction

Conclusions

References

Tables

Figures

◀

▶

◀

▶

Back

Close

Full Screen / Esc

Printer-friendly Version

Interactive Discussion

EGU

Stratospheric tracer modeling key aspects

B. Bregman et al.

Table 1. A summary of the model experiments. See text for more details for each experiment.

Experiment	advection	resolution	vertical layers	winds
“default” or “3×2”	2nd moments	3°×2°	45	6-hourly instantaneous
“red. grid”	2nd moments	3°×2°	45	6-hourly instantaneous
“slopes”	1st moments	3°×2°	45	6-hourly instantaneous
“30L”	2nd moments	3°×2°	30	6-hourly instantaneous
“1×1”	1st moments	1°×1°	45	6-hourly instantaneous
“6-hrly interp.”	2nd moments	3°×2°	45	6-hourly time interpolated
“3-hrly interp.”	2nd moments	3°×2°	45	3-hourly time interpolated

Title Page

Abstract

Introduction

Conclusions

References

Tables

Figures

◀

▶

◀

▶

Back

Close

Full Screen / Esc

Printer-friendly Version

Interactive Discussion

Stratospheric tracer
modeling key aspects

B. Bregman et al.

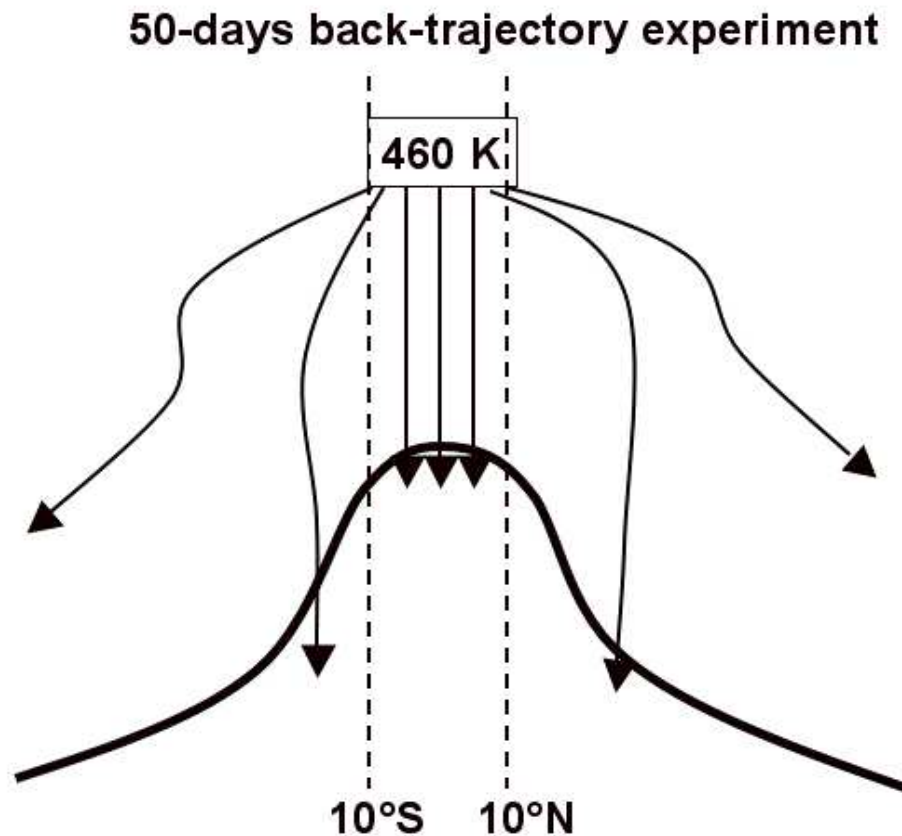


Fig. 1. A schematic view of the trajectory experimental setup. See text for more details.

[Title Page](#)[Abstract](#)[Introduction](#)[Conclusions](#)[References](#)[Tables](#)[Figures](#)[◀](#)[▶](#)[◀](#)[▶](#)[Back](#)[Close](#)[Full Screen / Esc](#)[Printer-friendly Version](#)[Interactive Discussion](#)

Stratospheric tracer
modeling key aspects

B. Bregman et al.

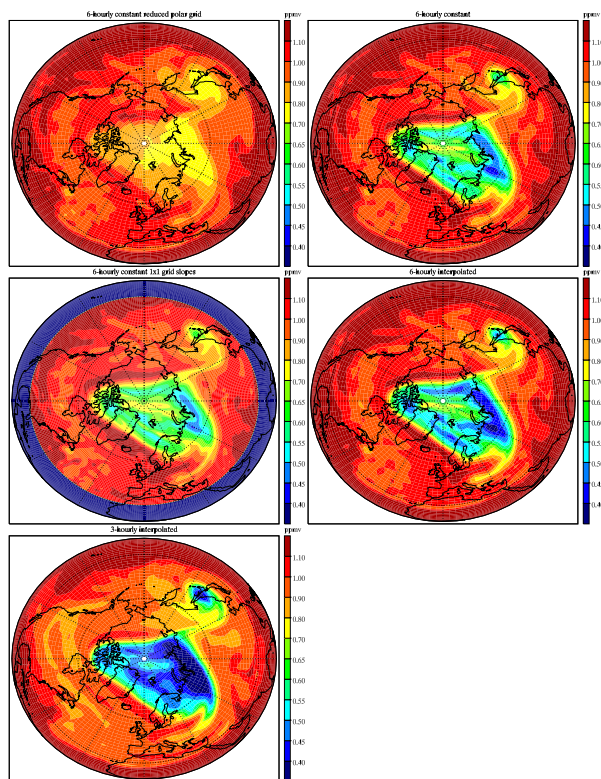


Fig. 2. Horizontal cross sections of methane mixing ratios (ppmv) at 35 hPa, 15 March 2000, 00:00 GMT for the “default”, “reduced grid” and “1×1” runs with 6-hourly instantaneous (constant) winds, and with the default configuration using 6-hourly and 3-hourly interpolated winds.

[Title Page](#)[Abstract](#)[Introduction](#)[Conclusions](#)[References](#)[Tables](#)[Figures](#)[I◀](#)[▶I](#)[◀](#)[▶](#)[Back](#)[Close](#)[Full Screen / Esc](#)[Printer-friendly Version](#)[Interactive Discussion](#)

Stratospheric tracer
modeling key aspects

B. Bregman et al.

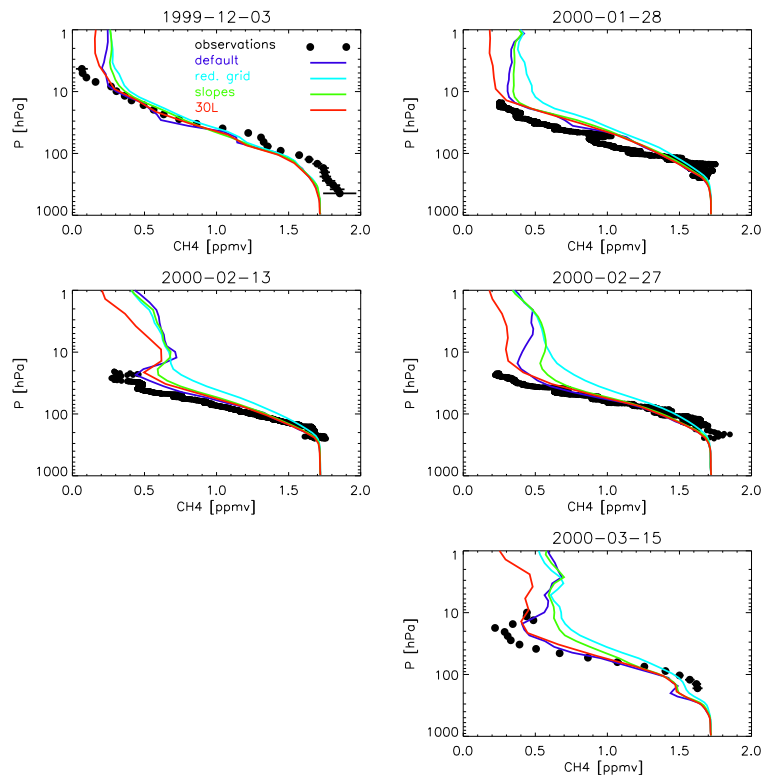


Fig. 3. Methane profiles (ppmv) versus pressure (hPa), observed (black dots), and calculated by the model (solid lines) at 15 March 2000. The horizontal bars denote the $2\text{-}\sigma$ observational uncertainty. Different model versions were used: “default” (blue), “red. grid” (light blue) “slopes” (green) is the default model setup but with a first-order advection scheme. “30L” (red) represents a twice as coarse vertical resolution in the stratosphere compared to “default”.

[Title Page](#)[Abstract](#)[Introduction](#)[Conclusions](#)[References](#)[Tables](#)[Figures](#)[◀](#)[▶](#)[◀](#)[▶](#)[Back](#)[Close](#)[Full Screen / Esc](#)[Printer-friendly Version](#)[Interactive Discussion](#)

Stratospheric tracer
modeling key aspects

B. Bregman et al.

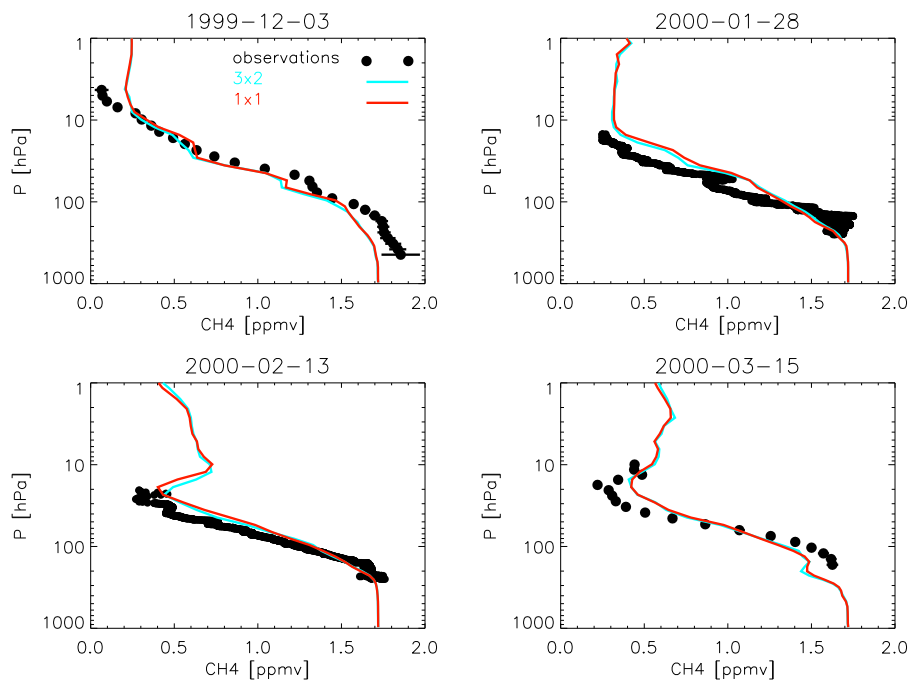


Fig. 4. As Fig. 3, but with the results from the default (blue) and “1 × 1” (red) runs. Day 2000-02-27 has been omitted.

[Title Page](#)[Abstract](#)[Introduction](#)[Conclusions](#)[References](#)[Tables](#)[Figures](#)[◀](#)[▶](#)[◀](#)[▶](#)[Back](#)[Close](#)[Full Screen / Esc](#)[Printer-friendly Version](#)[Interactive Discussion](#)

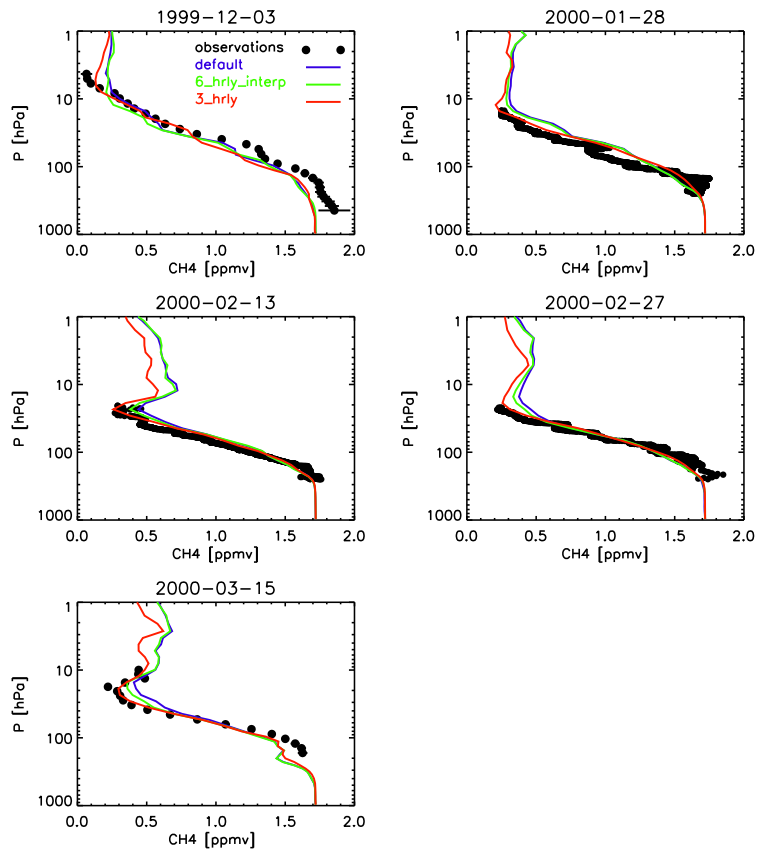


Fig. 5. As Fig. 3, but with the results from the default run (blue), using 6-hourly interpolated (green) and 3-hourly interpolated (red) winds. Day 2000-02-27 has been omitted.

Stratospheric tracer modeling key aspects

B. Bregman et al.

Title Page

Abstract Introduction

Conclusions References

Tables Figures

◀ ▶

◀ ▶

Back Close

Full Screen / Esc

Printer-friendly Version

Interactive Discussion

Stratospheric tracer modeling key aspects

B. Bregman et al.

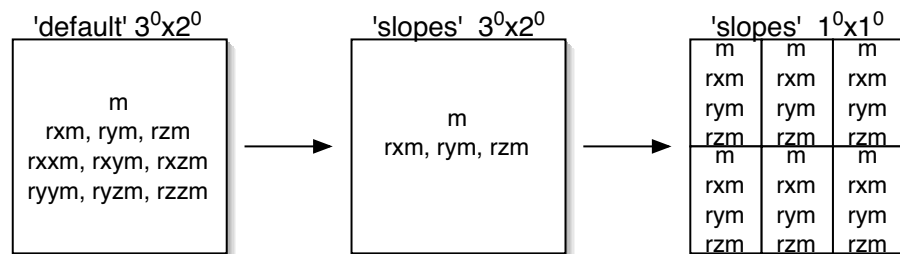


Fig. 6. A schematic view of the tracer information per grid cell of $3^\circ \times 2^\circ$, when applying second-moments (left) and first-order advection without grid zooming (middle) and with grid zooming (right).

Title Page

Abstract

Introduction

Conclusions

References

Tables

Figures

◀

▶

◀

▶

Back

Close

Full Screen / Esc

Printer-friendly Version

Interactive Discussion

EGU

Stratospheric tracer
modeling key aspects

B. Bregman et al.

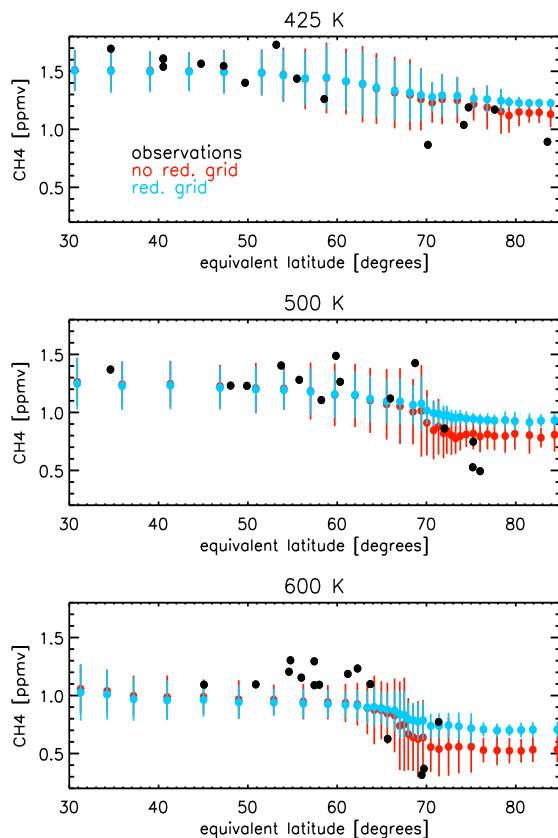


Fig. 7. Observed methane profiles volume mixing ratios in ppmv (black dots) at 15 March 2000, 00:00 GMT, and calculated by the model with the default model setup, with (red dots) and without (blue dots) the reduced polar grid. The comparison is performed at equivalent latitude (degrees) and three different isentropic levels (425 K, 500 K, and 600 K). The vertical bars represent 2σ variability of the model results.

[Title Page](#)[Abstract](#)[Introduction](#)[Conclusions](#)[References](#)[Tables](#)[Figures](#)[◀](#)[▶](#)[◀](#)[▶](#)[Back](#)[Close](#)[Full Screen / Esc](#)[Printer-friendly Version](#)[Interactive Discussion](#)

Stratospheric tracer
modeling key aspects

B. Bregman et al.

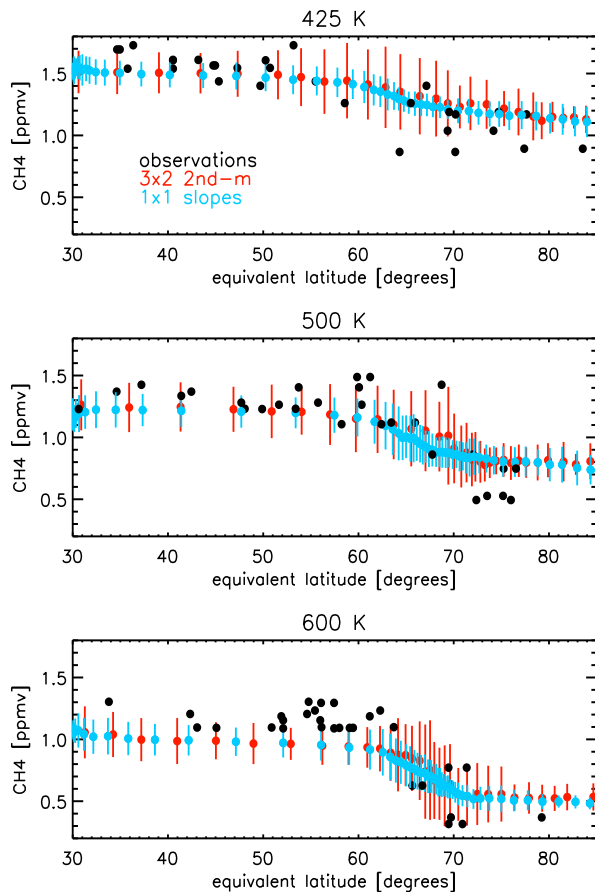


Fig. 8. Similar as Fig. 7, but with the results from the default (red dots) and “1 × 1” (blue dots) runs.

[Title Page](#)[Abstract](#)[Introduction](#)[Conclusions](#)[References](#)[Tables](#)[Figures](#)[◀](#)[▶](#)[◀](#)[▶](#)[Back](#)[Close](#)[Full Screen / Esc](#)[Printer-friendly Version](#)[Interactive Discussion](#)

Stratospheric tracer
modeling key aspects

B. Bregman et al.

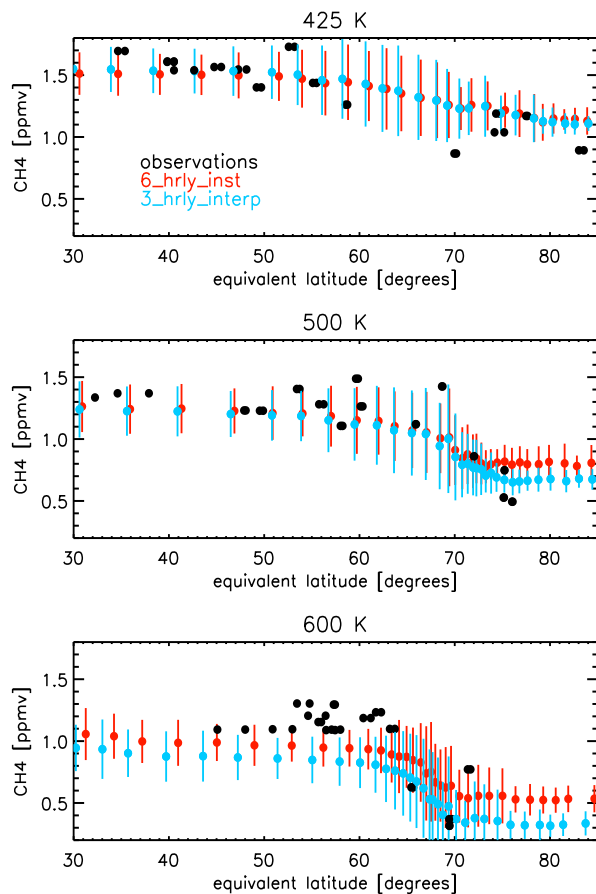


Fig. 9. Similar as Fig. 7, but with the results from the runs with the 3-hourly (blue dots) and 6-hourly (red dots) interpolated winds.

[Title Page](#)[Abstract](#)[Introduction](#)[Conclusions](#)[References](#)[Tables](#)[Figures](#)[◀](#)[▶](#)[◀](#)[▶](#)[Back](#)[Close](#)[Full Screen / Esc](#)[Printer-friendly Version](#)[Interactive Discussion](#)

EGU

Stratospheric tracer
modeling key aspects

B. Bregman et al.

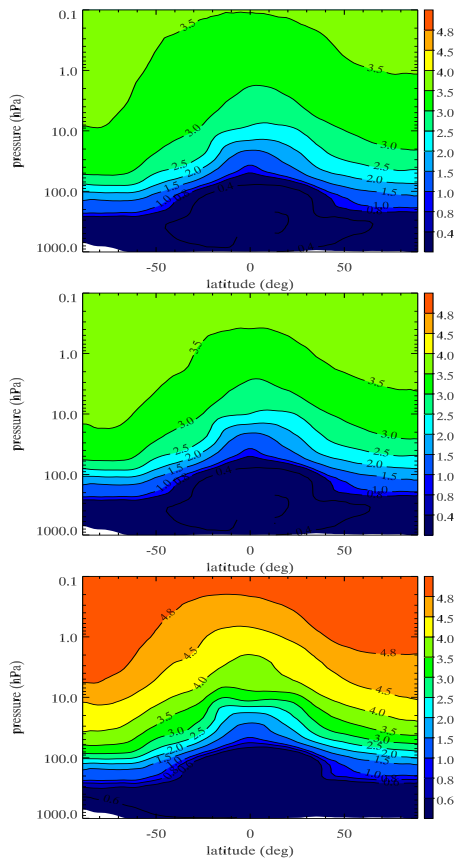


Fig. 10. Calculated latitudinal cross section of zonally average mean age of air (years) for three different experiments with second-order moments advection and without a reduced polar grid: using 6-hourly instantaneous (top panel), 6-hourly interpolated (middle panel) and the 3-hourly interpolated winds (bottom panel) respectively.

[Title Page](#)[Abstract](#)[Introduction](#)[Conclusions](#)[References](#)[Tables](#)[Figures](#)[◀](#)[▶](#)[◀](#)[▶](#)[Back](#)[Close](#)[Full Screen / Esc](#)[Printer-friendly Version](#)[Interactive Discussion](#)

Stratospheric tracer
modeling key aspects

B. Bregman et al.

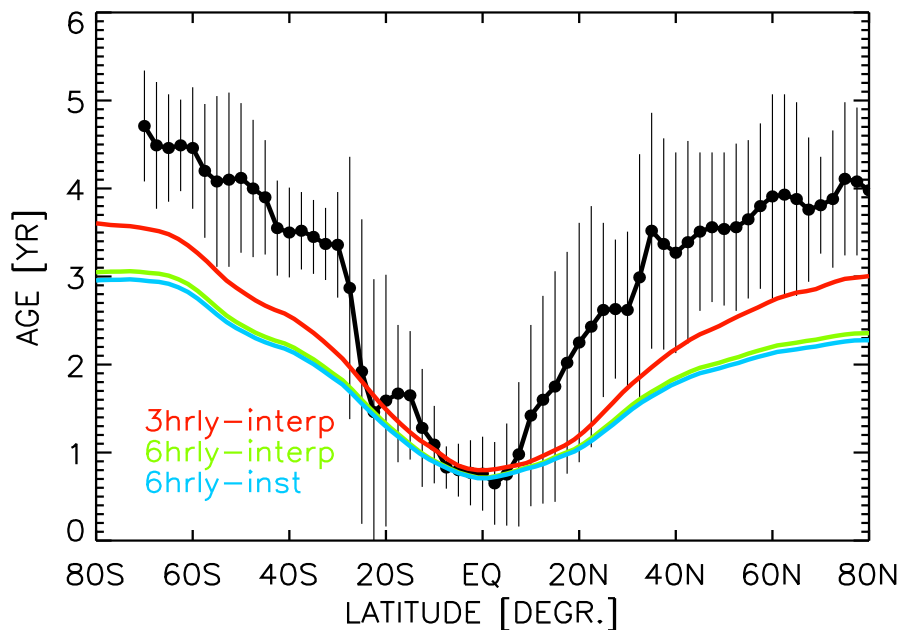


Fig. 11. Observed and calculated mean age of air for the same experiments as in Fig. 10. The observations (black dots) are derived from multi-year CO₂ observations from the ER-2 at approximately 20 km altitude (Andrews et al., 2001). The error bars represent 2- σ standard deviation.

[Title Page](#)[Abstract](#)[Introduction](#)[Conclusions](#)[References](#)[Tables](#)[Figures](#)[◀](#)[▶](#)[◀](#)[▶](#)[Back](#)[Close](#)[Full Screen / Esc](#)[Printer-friendly Version](#)[Interactive Discussion](#)

EGU

**Stratospheric tracer
modeling key aspects**

B. Bregman et al.

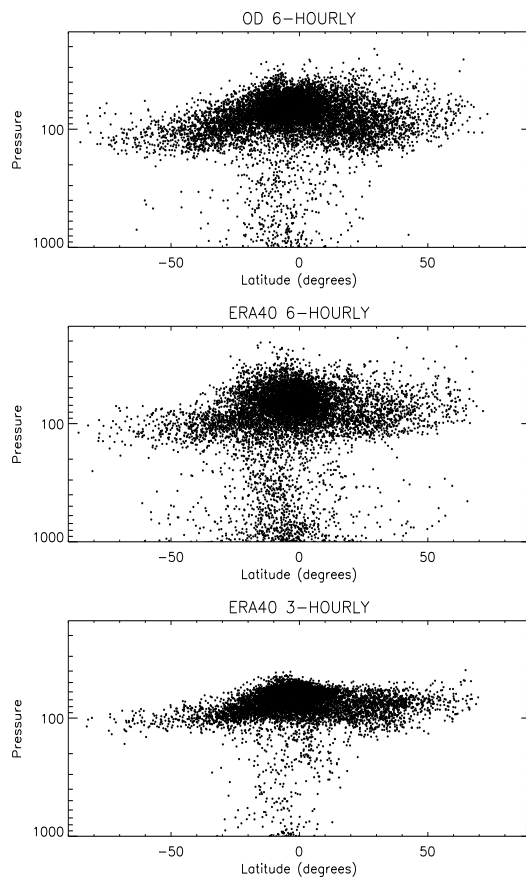


Fig. 12. The end locations of the air parcels after 50 days back-trajectory calculations for OD data with 6-hourly interpolated winds, ERA40 6-hourly and ERA40 3-hourly winds versus pressure and latitude.

[Title Page](#)[Abstract](#)[Introduction](#)[Conclusions](#)[References](#)[Tables](#)[Figures](#)[◀](#)[▶](#)[◀](#)[▶](#)[Back](#)[Close](#)[Full Screen / Esc](#)[Printer-friendly Version](#)[Interactive Discussion](#)

**Stratospheric tracer
modeling key aspects**

B. Bregman et al.

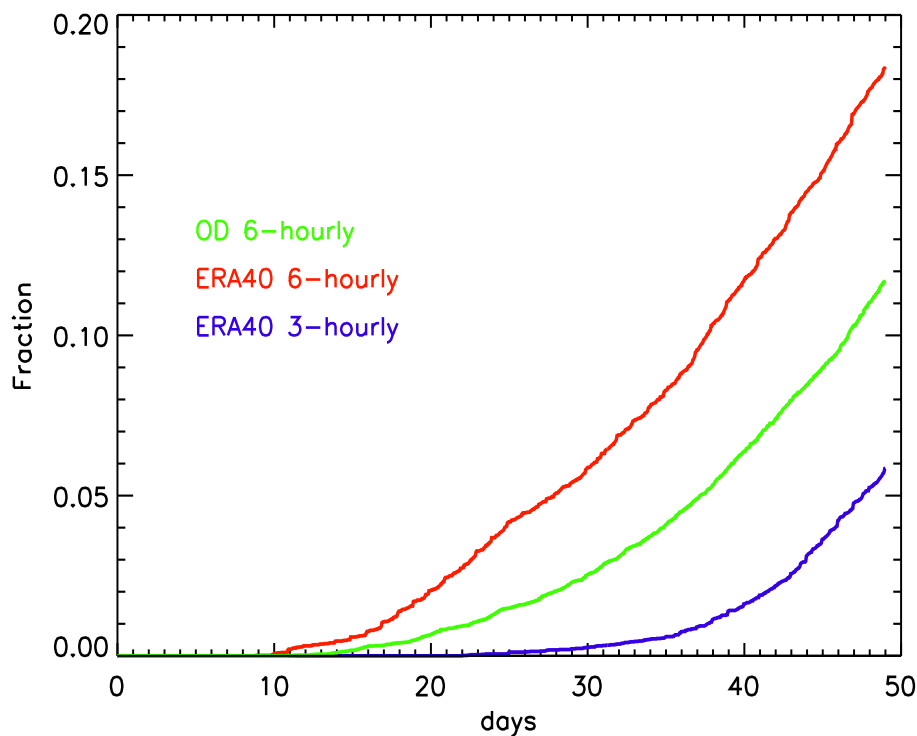


Fig. 13. The fraction of air parcels crossing the 10° S and 10° N border before moving through the tropopause for the same DAS winds as in Fig. 12: the OD data with 6-hourly interpolated winds (green line), and with ERA40 6-hourly (red line) and 3-hourly (blue line) interpolated winds respectively.

[Title Page](#)[Abstract](#)[Introduction](#)[Conclusions](#)[References](#)[Tables](#)[Figures](#)[◀](#)[▶](#)[◀](#)[▶](#)[Back](#)[Close](#)[Full Screen / Esc](#)[Printer-friendly Version](#)[Interactive Discussion](#)